Available online at www.sciencedirect.com
ScienceDirect
Journal of Power Sources 164 (2007) 721–729
JOURNAL OF POWER SOURCES
www.elsevier.com/locate/jpowsour

Three-dimensional heat and mass transfer analysis in an air-breathing proton exchange membrane fuel cell

Ying Wang *, Minggao Ouyang

State Key Laboratory of Automotive Safety and Energy, Tsinghua University, Beijing 100084, PR China

Received 30 September 2006; received in revised form 14 November 2006; accepted 17 November 2006
Available online 29 December 2006

Abstract

There is strong interaction between heat/mass transfer and electrode dynamics in an air-breathing proton exchange membrane fuel cell (PEMFC). To investigate the heat/mass transfer characteristics of PEMFC, their effect on oxygen transport and then on the performance of the cell, a coupled three-dimensional (3D) mathematical model has been developed for an air-breathing PEMFC using non-dimensional heat/mass transfer coefficients, and a detailed interpretation of heat/mass transfer parameters in it has been done. The full elliptic Navier Stokes and energy equations are simultaneously solved in the composite domain with commercial CFD tool STAR-CD based on the finite volume numerical method. And the model has been confirmed by experimental results. From the numerical simulation results obtained, a simple equation has been suggested on the function of the sum of Grashof number and diffusional Grashof number for the calculation of dimensionless mass transfer coefficient Sherwood number. The equation is believed to be useful for a profound understanding of the nature of oxygen transport limitation coupled with the heat/mass transfer in the air-breathing PEMFC, and further for the optimum design of the air-breathing PEMFCs. The concentration over-potential as a function of limited oxygen mass transfer rate, as well as profiles of velocity, temperature, reactant and water concentration, current density are presented and discussed to analyze the coupling problems between heat/mass transfer and electrode dynamics in an air-breathing PEMFC.

Keywords: Air-breathing; PEMFCs; CFD; Heat and mass transfer; Oxygen transport limitation

1. Introduction

Due to high electrical efficiency, flexibility with respect to power and capacity, long lifetime and good ecological balance, fuel cells have become one of the most interesting alternatives for clean power production in automotive applications and for distributed power generation. In addition to fuel cells for stationary or automotive applications, fuel cells also have the potential to complement or to substitute batteries in portable applications. The air-breathing PEMFCs operating at an ambient temperature without humidifier and air compressor are one of the most likely candidates for miniature fuel cells. A typical structure and principle of an air-breathing PEMFC that is used in our laboratory are illustrated in Fig. 1.

In this single air-breathing PEMFC, the structure consists of seven components as shown in Fig. 1. The electrolyte used here is Nafion 112, and the catalyst is platinum supported carbon. With two electrodes, the electrolyte and catalyst are assembled into a sandwich structure to form membrane-electrode-assembly (MEA). The cathode bipolar plate is machined to straight channel and anode plate designed as serpentine groove as shown in Fig. 1.

It has been known that the oxygen transport limitation plays a great role in the performance of air-breathing fuel cells from literatures [1–3]. In the air-breathing PEMFC, air flow into channel is driven by the effect of buoyancy, which is distributed throughout the air and is associated with the tendency of air to expand when heated. Air is heated due to irreversible losses when the electrochemical reaction occurs in the catalyst interface. The heated air becomes less dense and flows upwards. This process is called free convection. Thus the temperature gradient and electrochemical reaction has a remarkable impact on air flow rate. In addition, the liquid water also has a significant impact on the oxygen transport by blocking the gas way in the channel and backing layer when the air-breathing PEMFC works in high ambient humidity. The cell performance is decreased

* Corresponding author. Tel.: +86 10 62785706; fax: +86 10 62785708.
E-mail address: wangying@mail.tsinghua.edu.cn (Y. Wang).

0378-7753/$ – see front matter © 2006 Elsevier B.V. All rights reserved.
doi:10.1016/j.jpowsour.2006.11.056

Nomenclature

a	constant of the binary diffusion coefficient
A_{CV}	specific area of control volume (m^{-1})
b	exponent of the binary diffusion coefficient
$C_{O_2}^{\infty}$	oxygen concentration in ambient air ($kg\,m^{-3}$)
D	mass diffusion coefficient ($cm^2\,s^{-1}$)
F	Faraday's constant (96,487 C mol^{-1})
g	gravity ($9.8\,m\,s^{-2}$)
I	local current density ($A\,cm^{-2}$)
I_{lim}	concentration limiting current density ($A\,cm^{-2}$)
I^0	exchange current density ($A\,cm^{-2}$)
K	thermal conductivity ($J\,s^{-1}\,m^{-1}\,{}^oC^{-1}$)
K_P	the permeability of the porous medium (m^{-2})
l	characteristic length (m)
M	molecular weight of gases ($kg\,mol^{-1}$)
$\dot{m}_{O_2}$	oxygen mass flux in cathode catalyst surface ($kg\,m^{-2}\,s^{-1}$)
n_d	electro-osmotic drag coefficient
P	pressure (Pa)
P_{cr}	critical pressure (atm)
R	gas constant ($8.314\,J\,mol^{-1}\,K^{-1}$)
S	source term in governing equation
T	temperature (K)
T_{cr}	critical temperature (K)
t_D	diffusion layer thickness (mm)
t_{mem}	membrane thickness (mm)
$\vec{u}$	fluid velocity vector ($m\,s^{-1}$)
V_C	cell voltage (V)
$V_{intrinsic}$	intrinsic average velocity ($m\,s^{-1}$)
V_{oc}	open circuit voltage (V)
w	mass fraction

Greek letters

α	net water molecules per proton flux
β_T	coefficient of thermal expansion (T^{-1})
ε	porosity for a porous medium
η	over-potential (V)
μ	dynamic viscosity ($kg\,m^{-1}\,s^{-1}$)
∇	change in ...
ρ	gas phase density ($kg\,m^{-3}$)

Superscripts, subscripts

a	anode
act	activation
c	cathode
H_2	hydrogen
H_2O	water
m	gas mixture
mem	membrane
ohm	ohmic losses
O_2	oxygen
w	wall
0	initial condition

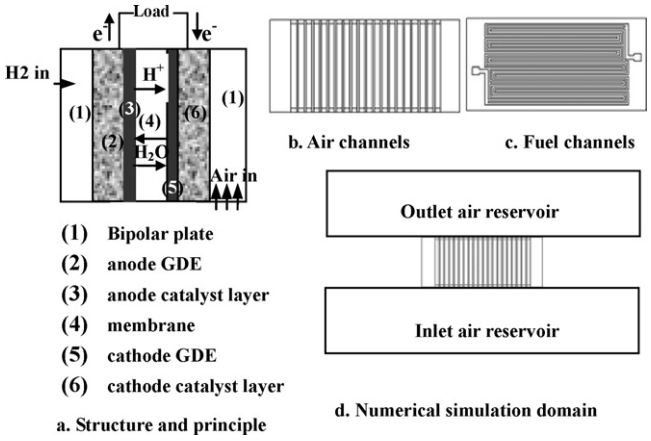

Fig. 1. Scheme of geometry and calculation domain of an air-breathing PEMFC.

extraordinarily when the oxygen partial pressure is insufficient in catalyst layer. Therefore, the performance of an air-breathing PEMFC is greatly influenced by heat/mass transfer as well as air free convection and water transport. And all these processes are very closely coupled. Understanding these transport processes and the effects of them on the performance of electrochemical reaction in an air-breathing PEMFC is evidently important for optimization of the fuel cell design and operating conditions. Hence a comprehensive modeling of these processes is an effective way of doing optimization.

Many models focused on general forced convection PEMFC, most of them are one-dimensional (1D) flows, Springer and his co-workers developed an isothermal, one-dimensional, diffusion model. At the same time, Bernardi and Verbruge [4] developed a heat and water management model in dimensions normal to the reactive interface. Nguyen and Springer [5,6] developed a one-dimensional mathematical model in dimensions along the channel. One-dimensional models restrain the application to simple geometry and isothermal assumption even though they have provided useful insight and fundamental understanding. To predict the performance of fuel cells, to investigate the operation of fuel cells and to optimize the distribution of gas, two-dimensional and three-dimension models were developed recently. Hsing and Futerko [7] developed a two-dimensional model of coupled fluid flow, mass transport and electrochemistry of PEMFC operating without external humidification of hydrogen and air streams. Dutta [8,9] described a steady state, isothermal, three-dimensional and single phase PEMFC model used to predict the performance of a fuel cell. In addition, recently there are several works about heat/mass transfer, and air-breathing PEMFCs have been published. Jeong et al. [10] investigated the characteristics and optimized the cathode structure of air-breathing PEMFCs through experiment. And the influence of gas diffusion layer properties and cathode catalyst loading on the cell performance are examined in their works. Further, in their another literature [11], they investigated experimentally the effects of cathode open area and relative humidity on the air-breathing fuel cell performance, and found that the single cell with the open area of 77% exhibited the highest performance. Ramousse et al. [12] presented a fuel cell model

in the condition of forced convection considering gas diffusion in porous electrodes, water diffusion, electro-osmotic transport through the polymeric membrane and heat transfer in both the membrane electrodes assembly (MEA) and bipolar plates. The results showed that thermal gradients in the MEA could lead to thermal stresses at high current densities. Arato and Costa [13] discussed the interaction between diffusive and forced flows expressed in terms of Peclet numbers and the overall diffusive resistance in terms of Sherwood numbers in a forced convection PEMFCs with emphasis on the oxygen diffusion limitation. The results of this approach were then used in the discussion of the performance of different geometric arrangements, such as traditional, interdigitated and serpentine cells. Shan and Choe [14] presented a dynamic PEMFCs stack model taking into account heat transfer, and analyzed start-up behaviors and the performance of the stack. Wang et al. [15] developed a two-dimensional numerical model for an air-breathing PEMFC including water transportation and electrochemical reaction in catalyst layer. In this model they discussed the effect of cathode open size on cell performance and suggested a best opening for the cathode channel.

In spite of the fact that the above-cited references have stressed the modeling and calculation for fuel cells to analyze the various phenomena, none of them addresses the full three-dimensional solution for heat/mass transfer, fluid dynamics and electrochemistry in an air-breathing PEMFC. It is extremely challenging to derive and to solve those kinds of strongly coupled model equations. In previous studies, Wang et al. [16,17] have investigated the effect of cathode plate configuration on cell performance by developing a three dimensional CFD model for an air-breathing PEMFC. Experimental data has also been collected to confirm the model result and the cell performance under different air humidity, the temperature on the carbon surface.

In this work, we developed a model that could analyze in detail the important characteristic of heat and mass transfer in an air-breathing PEMFC. A correlation between Sherwood number and Grashof number has been derived on the basis of the numerical results, and the correlation could greatly simplify the calculation of the limiting current density without the development and solution of a full N–S equation.

The computation domain comprised an actual physical domain between two bipolar plate, as well as two relatively large domains placed on the upstream of channel entrance and on the downstream of the channel exit as shown in Fig. 1. These I-type composite domains resemble open, unbounded spaces that serve to accommodate the diffusion phenomena by momentum and energy that could occur outside of the channel. Using computational fluid dynamics technique, the conservation equations have been solved using velocity, temperature, concentration of gas component, over-potential and current density fields to analyze the effect of heat and mass transfer on the performance of an air-breathing PEMFC with the perspective of its optimization.

2. Model descriptions

The air-breathing PEM fuel cell model presented here is a comprehensive three-dimensional, non-isothermal, steady state model for explaining the complicated process of heat and mass transfer, electrochemistry and fluid dynamics in an air-breathing PEMFC.

2.1. Model assumptions

A complete air-breathing PEMFC is an extremely complex system. Therefore, to obtain the solution of three-dimensional model of an air-breathing PEMFC it is necessary to do some reasonable simplifying assumptions. In this model following assumptions are used:

- The water exists in the fuel cell as vapor water. It is reasonable because the water partial pressure is not high in air-breathing PEM fuel cell without external humidification but with low ambient air humidity.
- Ohmic heating and ohmic resistance in the bipolar plate and in the carbon gas diffusion layer are neglected due to high thermal conductivity and electrical conductivity.
- Membrane is assumed to be solid for faster numerical convergence.

2.2. Governing equations

In the gas flow field, the flow is a laminar steady state flow. The governing equations of the fluid flow represent mathematical statements of the conservation laws of physics. Considering the effect of porous medium, from the Dupuit–Forchherimer relationship ($\vec{u} = \varepsilon V_{\text{intrinsic}}$) [18], the fluid conservation equations in porous medium can be derived as following. The detailed arguments can also be found in Wang's work [19].

2.2.1. Continuity equation

The mass conservation can be stated for steady state flow as following:

$$\nabla \cdot \varepsilon(\rho\vec{u}) = S_{\text{mass}} \tag{1}$$

ε is porosity for a porous medium, which is zero in channel and S_{mass} is the mass source or sink because of electrochemical reaction, which is sum of source terms for oxygen, nitrogen, vapor water in cathode and for hydrogen, vapor water in anode.

2.2.2. Momentum conservation

Following momentum equation is derived from Newton's second law:

$$\nabla \cdot (\rho\vec{u}\vec{u}) = -\nabla P + \nabla \cdot (\mu\nabla\vec{u}) + \rho g - \left(\frac{\varepsilon\mu\vec{u}}{K_{\text{P}}}\right) \tag{2}$$

Here the terms from left to right are, respectively, convective terms, pressure drop terms, diffusive terms, buoyancy effect terms according to Boussinesq approximation and terms for pressure drop due to small permeability of porous medium based on Dancy's law. K_{P} is the permeability of the porous medium. The dynamic viscosity of gas mixture can be calculated from following formula [20]:

$$\mu = \sum_{i=1}^{N} \frac{Y_i \mu_i}{\sum_j Y_j \varphi_{ij}} \tag{3}$$

where Y_i and Y_j are molar fraction of gas components i and j, μ_i is dynamic viscosity of gas component i, i and j represent either oxygen, nitrogen or vapor in cathode, and hydrogen or vapor in anode, the non-dimensional parameter φ_{ij} can be calculated from following formula [20]:

$$\varphi_{ij} = \frac{1}{\sqrt{8}} \left(1 + \frac{M_i}{M_j}\right)^{-1/2} \left[1 + \left(\frac{\mu_i}{\mu_j}\right)^{1/2} \left(\frac{M_j}{M_i}\right)^{1/4}\right]^2 \tag{4}$$

where M_i and M_j are molecular weight of gas components i and j.

2.2.3. Energy conservation

The energy equation is derived from the first law of thermodynamics:

$$\nabla \cdot \varepsilon \left(\rho c_P \vec{u} T\right) = \nabla \cdot \left(K^{\text{eff}} \nabla T\right) + S_T \tag{5}$$

Here K^{eff} is the effective thermal conductivity of gas mixture in porous medium, which can be yielded as a simple function of the gas mixture thermal conductivity in nonporous system. This approximate equation is derived from the analogue with the calculation of the effective diffusion coefficient to simplify the numerical process.

$$K^{\text{eff}} = K\varepsilon^{1.5} \tag{6}$$

c_P is the specific heat capacity at constant pressure and K is the thermal conductivity of gas mixture, which can be estimated with a function of the individual gas component's thermal conductivity weighted by the mass fraction from following formula according to the methodology of STAR-CD:

$$\phi = \sum_{i=1}^{N} w_i \phi_i \tag{7}$$

ϕ represents the specific heat capacity or the thermal conductivity of gas mixture, ϕ_i represents the specific heat capacity or the thermal conductivity of gas component i.

S_T is energy source term which represents the rate of increase or decrease of energy due to heat generations or consumptions. In the catalyst layer, because of the heat transformed from irreversible over-potential, the source terms in cathode and anode are, respectively:

$$S_T^{\text{a}} = A_{\text{CV}} I \eta_{\text{a}}, \quad S_T^{\text{c}} = A_{\text{CV}} I \eta_{\text{c}} \tag{8}$$

In membrane, heat generated from ohmic resistance.

$$S_T^{\text{mem}} = A_{\text{CV}} I \eta_{\text{ohm}} \tag{9}$$

Here A_{CV} is specific surface area of the control volume.

The momentum equation and energy equation are coupled via equation of state of ideal mixtures.

$$\rho = \frac{P M_{\text{m}}}{RT} \tag{10}$$

where M_{m} is the molecular weight of the gas mixture which can be calculated from mass fraction of gas component in gas mixture.

$$M_{\text{m}} = \frac{1}{\sum_i (w_i / M_i)} \tag{11}$$

where w_i is the mass fraction of gas component and M_i is the molecular weight of gas component i.

2.2.4. Species mass transport

The mass fraction of gas component can be calculated from following transport equation:

$$\nabla \cdot (\varepsilon \rho w_i \vec{u}) = \nabla \cdot (D_i^{\text{eff}} \nabla \rho w) + S_i \tag{12}$$

Here D_i^{eff} is effective molecular diffusion coefficient of gas component i in the porous medium and have a relationship with gas diffusion coefficient in nonporous material D_i as stated in literature [18]

$$D_i^{\text{eff}} = D_i \varepsilon^{1.5} \tag{13}$$

D_i can be calculated from binary diffusion coefficients.

$$D_i = \frac{(1/M_{\text{m}})(1 - w_i)}{\sum_{j \neq i} (w_j / D_{ij} M_j)} \tag{14}$$

where the binary diffusion coefficient D_{ij} for gas components i and j is calculated from Slattery and Bird estimation [20]

$$D_{ij} = \frac{10.13 \times a (T/\sqrt{T_{\text{cr},i} T_{\text{cr},j}})^b (P_{\text{cr},i} P_{\text{cr},j})^{1/3} (T_{\text{cr},i} T_{\text{cr},j})^{5/12} ((1/M_i) + (1/M_j))^{1/2}}{P} \tag{15}$$

The value of parameters used in above equation can be found in Table 1. According to Faraday's laws, the source term S_i in species mass transport equation for oxygen and hydrogen is:

$$S_r = \frac{-\text{IM}_r A_{\text{CV}}}{nF} \tag{16}$$

where r is oxygen or hydrogen, M_r the molecular mass weight of reactant r, n is 2 for hydrogen and 4 for oxygen.

Vapor water source term can be calculated from the balance of water transport. Vapor water source terms in anode and in cathode are:

$$S_{\text{H}_2\text{O}}^{\text{a}} = -\frac{M_{\text{H}_2\text{O}} A_{\text{CV}} \alpha}{F} \tag{17}$$

Table 1
The value of parameters used in the equation for binary diffusion coefficient

Species A	M_{A}	a_{AB}	b_{AB}	P_{cA}	T_{cA}	Species B
O_2	31.999	3.64E−4	2.334	49.7	154.4	H_2O
N_2	28.013	2.75E−4	1.823	33.5	126.2	O_2
H_2O	18.015	3.64E−4	2.334	221.2	647.3	N_2

$$S^{c}_{H_2O} = \frac{IM_{H_2O}A_{CV}}{2F} + \frac{\alpha M_{H_2O}A_{CV}}{F} \quad (18)$$

Here net water molecules per proton flux α can be yielded from following water transport equation through membrane:

$$\alpha = n_d - \frac{FD_w(C_{w,c} - C_{w,a})}{It_{mem}} \quad (19)$$

The first term in the right of the equation is water molecules from anode to cathode by electro-osmotic drag caused by proton transport. The second is the diffusion term of water molecules by concentration difference between anode and cathode side, based on a single-step linear water concentration difference assumption. $C_{w,c}$ and $C_{w,a}$ are, respectively, water concentrations in cathode and anode. The electro-osmotic drag coefficient n_d, and the water diffusion coefficient in membrane D_w can be obtained from the function of the water content in membrane. The detailed membrane model has been presented in literature [15].

The mass fraction of nitrogen can be obtained by

$$w_{N_2} = I - w_{O_2} - w^{c}_{H_2O} \quad (20)$$

In above equation, I is the current density that can be calculated from following equations [6,8]:

$$V_C = V_{OC} - \eta_{act} - \eta_{ohm} - \eta_{conc} \quad (21)$$

$$\eta_{act} = \frac{RT}{0.5F} \ln\left(\frac{I}{I^0 P_{O_2}}\right) \quad (22)$$

$$\eta_{ohm} = \frac{t_{mem} I}{\sigma_{mem}} \quad (23)$$

$$\eta_{conc} = -3.4 \times 10^{-4} T \ln\left(1 - \frac{I}{I_{lim}}\right) \quad (24)$$

Here the membrane conductivity σ_m can be obtained as a function of temperature and water content in membrane [9], the concentration over-potential η_{conc} is related to the oxygen transfer rate in the cathode channel. And then the limiting current density I_{lim} can be calculated from oxygen transport limitation according to literature [21].

$$I_{lim} = \frac{4FD_{O_2}C^{\infty}_{O_2}Sh}{t_D} \quad (25)$$

where the dimensionless mass transfer coefficient Sherwood number (Sh) is calculated by following equation based on the definition in literature [20]:

$$Sh = \frac{(t_D/D_{O_2})\dot{m}_{O_2}}{\rho(w^{\infty}_{O_2} - w_{O_2})} \quad (26)$$

2.3. Numerical scheme

The calculation procedure is carried out in commercial CFD tool STAR-CD with the parameters, boundary conditions and geometry dimension listed in Table 2. The initial source terms for governing equations are obtained from average current density and calculated over-potential at first sweep of iterations. The governing equations are solved based on the SIMPLE algorithm and the monotone advection and reconstruction scheme (MARS) using finite-volume approach. The partial pressure of gas component and the oxygen mass transfer coefficient are obtained from the solution and are used to calculate the current density, over-potential and the net water molecules per proton flux by user-defined subroutine based on the finite-difference discretization technique. Then with the new source terms calculated using newly obtained values the governing equations are solved iteratively until the convergence.

3. Results and discussions

In the following paragraph the results are presented for an air-breathing PEMFC operated in the condition shown in Table 2, with an electrode area of 34.4 cm^2, the anode and cathode channel arranged as intercross flow mode. The analysis has been made to investigate the effects of heat and mass transfer, water profile on the performance of the air-breathing PEMFC.

3.1. Model validation

The fuel cell terminal voltage was calculated for series of cell current density based on the operating conditions shown in Table 2. The experiment has been carried out in our laboratory with the same cell geometry specified to validate the calculated voltage values. Fig. 2 compares the calculated voltage for this air-breathing PEMFC as a function of current density with the experiment results. Generally the computed voltages for several current densities shown in Fig. 2 are in good agreement with the experimental data. However, the calculated performance is little higher than the experimental result. This discrepancy is believed to be due to the experimental errors

Table 2
Values for parameters and boundary condition used in the model

Parameters	Symbol	Value	Parameters	Symbol	Value
Porosity in carbon paper and catalyst layer	ε	0.4, 0.28	Cathode channel height and width	h_c, w_c	0.3 cm
Average current density	I_{avg}	0.15 A cm^{-2}	Relative humidity in air	ξ	63% RH
Ambient temperature, pressure	T_b, P	300 K, 101,325 Pa	Membrane thickness	t_m	0.0508 mm
Anode channel width, height	w_a, h_a	0.1 cm	Thickness of Diffusion layer, catalyst layer	t_d, t_s	0.026 mm, 0.001 mm
H_2 inlet temperature	T_a	299 K	Oxygen/nitrogen ratio in air	ζ	0.21/0.79
H_2 flow rate in inlet	N_{H_2}	7.198E−08 kg s^{-1}	Cathode channel length	L_c	47 mm
Permeability in GDL	K_P	1.8E−18 m^2	Permeability in catalyst layer	K_P	1.76E−12 m^2

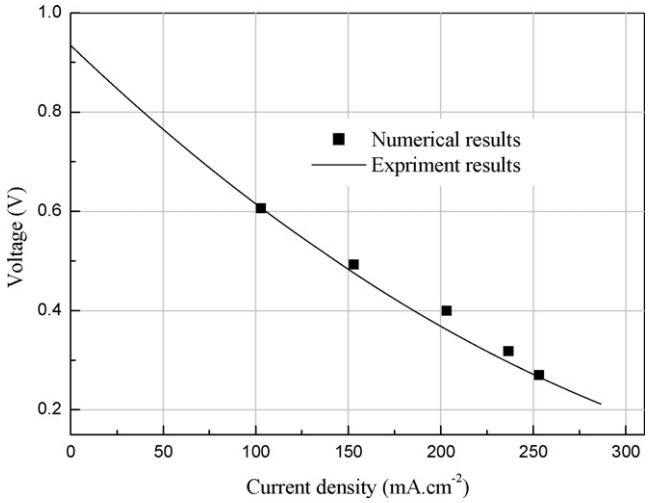

Fig. 2. Comparison of polarization curves between the numerical prediction and experimental results.

caused by difficulties in controlling of ambient humidity and temperature.

3.2. Effect of heat transfer

To understand the effect of the heat transfer, the calculated profiles of temperature, Grashof number (Gr_T), velocity and current density are presented here at the current density of 0.15 A cm^{-1}, which is estimated to be an optimal operation current load from Fig. 2.

Fig. 3 displays the temperature profile in the MEA region. Because of low thermal conductivity in the diffusion layer and a low heat transfer coefficient in catalyst layer, the gas temperature in the catalyst layer is the highest. Given the temperatures in the cathode and anode diffusion layer in the figure, those temperature profiles in this air-breathing PEMFC is different from those of general forced convection PEMFC where the temperature of the anode is a little higher than in cathode. This is apparently due to the fact that in an air breathing PEMFC, the cathode, which has an air channel, can release more heat to the ambient air than the anode. Observing the temperature distribution in the catalyst interface, the temperature is high in the center due to the presence of thermal diffusion and convection in the air channel. And the temperature is high in the region near the anode inlet and outlet because there is a strong electrochemical reaction caused by affluent hydrogen or water. The region near

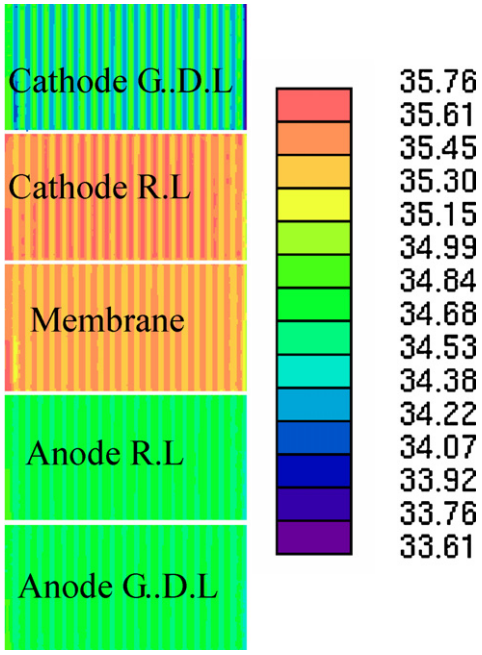

Fig. 3. Temperature distribution in different layers of MEA (°C).

the outlet of the anode should be rich of water because of continuous water generation from electrochemical reaction. For this air-breathing PEMFC operated under low humidity condition, higher water concentration could be better for electrochemical reaction. Fig. 4 shows the temperature profile of the cathode channel. The thermal boundary layer can be clearly observed. In the air-breathing PEMFC, air is heated from the bottom near the MEA surface, the heat transfer includes the heat transport from the MEA to the air channel and to the solid plate by convection and conduction, and the heat transport between air in the channel and solid plate. To simplify the model the heat transfer resistance between different regions was not taken into account. Evidently there should be a trade-off between the heat transfer to solid plate and to air in the channel in order to improve the free convection in the channel. But it is difficult to give a clear definition to the optimal ratio for the heat transfer rate between to air and to solid plate due to coupled effects between these two. However, in the air-breathing PEMFC, what is more important than the heat transfer itself is the mass transfer rate that is limiting the performance of the cell. The heat transfer put an important effect on the mass transfer through the buoyancy forces. The dimensionless parameter Grashof number defined

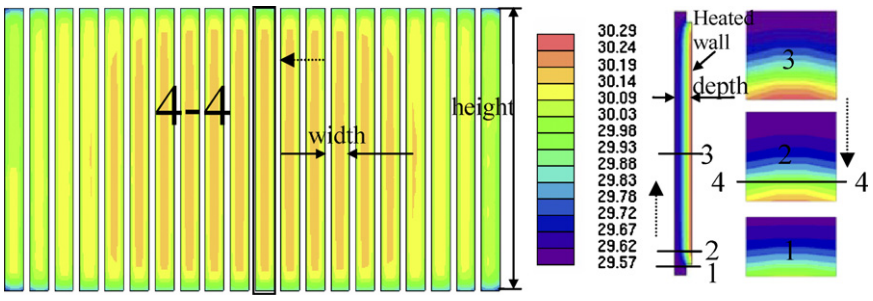

Fig. 4. Temperature distribution in cathode channel (°C) (⋯▶ is the view direction for the section plot).

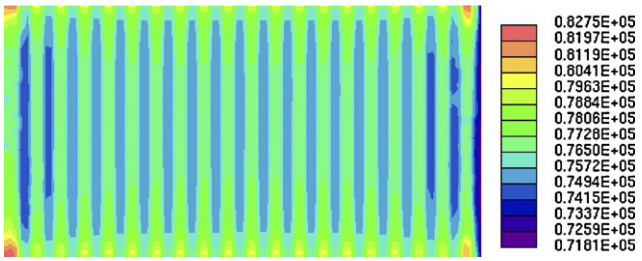

Fig. 5. The distribution of local Grashof number in cathode catalyst surface.

as the strength of buoyancy effect due to temperature difference could greatly contribute to the mass transfer rate in the air breathing PEMFC. Fig. 5 shows the distribution of local Grashof number. According to Bird et al. [20], the Grashof number can be calculated from a simple formula,

$$Gr_T = \frac{g\beta_T \rho^2 (T_w - T_0) l^3}{\mu^2} \quad (27)$$

The distribution of the Gr_T is not uniform due to uneven electrochemical reaction. Comparing Figs. 3–5, it can be observed that the heat transfer takes place almost throughout the full length of the channel. And in the middle of plate, in the opening of the furthest right and left channel near the anode inlet and outlet, the heat transfer has a significant effect on free convection of the air. This also can be proved from the profile of velocity shown in Fig. 6. The center channels have a longer entrance length than others. The flow is not developed yet and shows strong mass and heat transfer in the entrance region. In the middle channel marked by '3' in the figure has longest entrance length. In the channels, marked '1', '2' in the figure, air flows into channel not only from the bottom inlet but also from the top opening due to characteristic of heat transfer and electrochemical reaction. Fig. 7 shows the current density distribution. Similarly the electrochemical reaction is increased in the channels '1' and '2', and the regions near the opening of the cathode channel. From Figs. 3–7, it can be observed that there exsits strong interaction between heat transfer and electrochemical reaction. Effective heat transfer in the air channel can improve the performance of air-breathing PEMFC by causing uniform gas distribution, and by sustaining a good heat transfer rate between solid and fluid, and observed in the long thermal and velocity entrance length in the cathode channel.

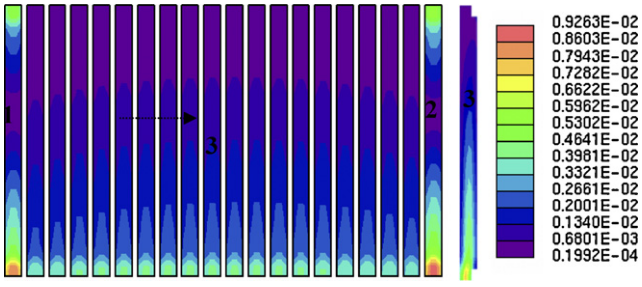

Fig. 6. The velocity profile in cathode channel, m s^{-1}.

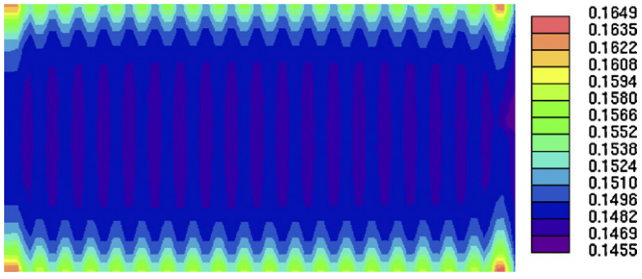

Fig. 7. The current density distribution in catalyst surface, A cm^{-2}.

3.3. Effect of mass transfer

The performance of air-breathing PEMFCs is strongly affected by free convection in air channel. When air supply to channel is not sufficient, the oxygen partial pressure in the catalyst layer is accordingly low; the performance of cell decreased by the function of Nernst equation, this phenomenon is called mass transport limitation losses or concentration losses. If the oxygen concentration is less than some level in catalyst layer, the cell will stop working completely. Fig. 8 is oxygen mass fraction distribution in cathode side. It shows that the oxygen mass fraction is much lower than in ambient air even though the cell works in such low current load. The calculated air mass flux to catalyst layer by convection is 6.818E−7 kg s^{-1}, and hence approximately, 1.32E−7 kg s^{-1} oxygen flows into catalyst layer by convection considering the oxygen mass fraction in air. Moreover, there is a little oxygen diffusion to catalyst layer. Total oxygen supply should sustain the electrochemical reaction at this average current density. The air-breathing PEMFCs can not work at high current density because of limited oxygen supplement. The current density at which the oxygen is used up is called limiting current density where the cell cannot work beyond. In the air-breathing PEMFC, the limiting current

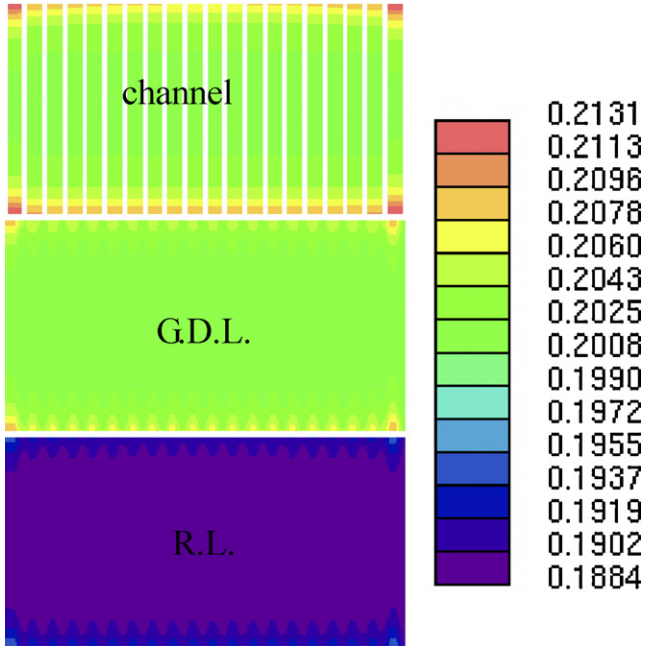

Fig. 8. Oxygen mass fraction in cathode side (G.D.L. is abbreviation of diffusion layer, R.L. is abbreviation of catalyst layer).

density is closely associated with mass transfer rate to catalyst layer. The mass transfer in the air-breathing PEMFC is decided not only by free convection related to heat transfer, but also by the oxygen diffusion caused by concentration gradients at the electrochemical reaction zone. Similar to the heat transfer, the diffusional Grashof number due to concentration difference can be derived as following for mass transfer [20]:

$$Gr_{\mathrm{M}} = \frac{g\gamma\rho^2(w_{\mathrm{O_2,w}} - w_{\mathrm{O_2},0})l^3}{\mu^2} \tag{28}$$

As thermal coefficient of volume expansion in free convection heat transfer, mass expansion coefficient is

$$\gamma_{\mathrm{O_2}} = -\left(\frac{1}{\rho}\right)\left(\frac{\partial\rho}{\partial w_{\mathrm{O_2,w}}}\right)_P \tag{29}$$

For mass transfer between three ideal gases, the expression for them can be further derived as

$$\gamma_{\mathrm{O_2}} = \frac{M_{\mathrm{H_2O}}M_{\mathrm{N_2}} - M_{\mathrm{H_2O}}M_{\mathrm{O_2}}}{M_{\mathrm{H_2O}}M_{\mathrm{N_2}}w_{\mathrm{O_2,w}} + M_{\mathrm{O_2}}M_{\mathrm{N_2}}w_{\mathrm{H_2O,w}} + M_{\mathrm{O_2}}M_{\mathrm{H_2O}}(1 - w_{\mathrm{H_2O,w}}. - w_{\mathrm{O_2,w}})} \tag{30}$$

Fig. 9 shows the distribution of diffusional Grashof number. On the contrary to heat transfer, in the right and left furthest channel, the diffusional Grashof numbers are low due to small concentration differences. Therefore, considering the heat transfer and mass transfer simultaneously, it can be found that the mass transfer rate is affected by the combination of heat transfer and mass transfer. Considering the heat transfer and mass transfer by the free convection in the channel and in the porous medium, there are few equations applicable till now especially for mass transfer rate in this case. Literature [20] derives it from analogy of heat transfer coefficient. However, more reasonable values could be derived from the air flow rate which can be calculated from solution of full Navier–Stokes equation.

Fig. 10 shows the Sherwood number distribution, which represents the oxygen transport characteristic in cathode. Comparing with current density distribution in Fig. 7, it is found that these two figures have very similar pattern. Therefore, it can be concluded that the mass transport plays major role in cell performance. Comparing the profiles for Grashof number and diffusional Grashof number with those of Sherwood number distribution, it can evidently be found that the free convection due to temperature difference and the diffusion due to concentration gradients has great impact on the oxygen transport, and

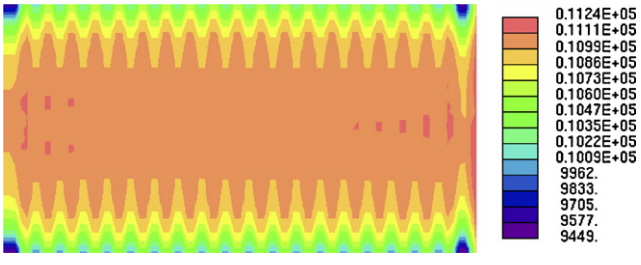

Fig. 9. The distribution of diffusional Grashof number in cathode catalyst surface.

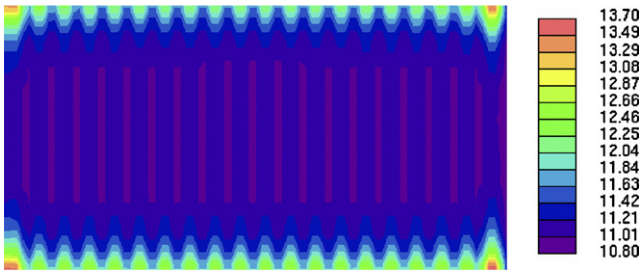

Fig. 10. Sherwood number distribution in cathode catalyst surface.

there are some coupled relationships between the Sh and Gr_{m}, Gr_{T}. Therefore, it is more desirable that Sh is calculated by the solution of full N–S equation, however, the complexity and difficulties encountered to solve the equation limited the application of this method. Therefore, it is necessary to develop a simple equation to calculate the Sh. A correlation of Sh and Gr_{m}, Gr_{T} has been suggested for the vapor natural convection model including heat and mass transfer simultaneously [20].

$$Sh = C_1(C_2(Gr_{\mathrm{m}} + Gr_{\mathrm{T}})^{1/4}) \tag{31}$$

where the coefficient C_1 is 0.518 and C_2 is 0.61.

The problem in our work is similar to that described in literature [20], therefore, it can be derived that the Sherwood number is function of the sum of Grashof number and diffusional Grashof number based on above formula and our numerical results.

$$Sh = 0.65(Gr_{\mathrm{m}} + Gr_{\mathrm{T}})^{1/4} \tag{32}$$

This equation figures out the essential factors that influent the oxygen transport, and helpful to understand the interaction of heat/mass transfer and dynamics inside the cell. Using the equation, the oxygen transport coefficient can be easily calculated, and then limiting current density can be obtained very simply. In addition, Sherwood number calculated from above equation can also be used to evaluate if the configuration of the cell is reasonable and to optimize the oxygen transportation in the cell.

Fig. 11 shows concentration losses caused by oxygen insufficiency. The reduction of cell performance due to oxygen transport limitation is shown to be proportional to oxygen transfer coefficient.

3.4. Effect of water transport

Generally the water management is vital problem for any fuel cells. However, the water transport through the membrane for

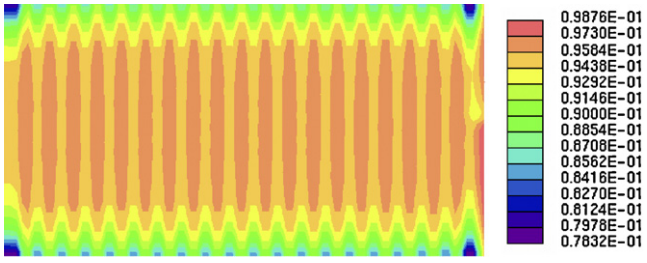

Fig. 11. Concentration over-potential distribution in catalyst surface.

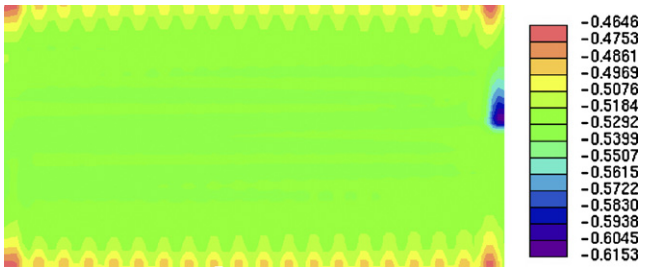

Fig. 12. Distribution of net water molecules per proton flux through the membrane.

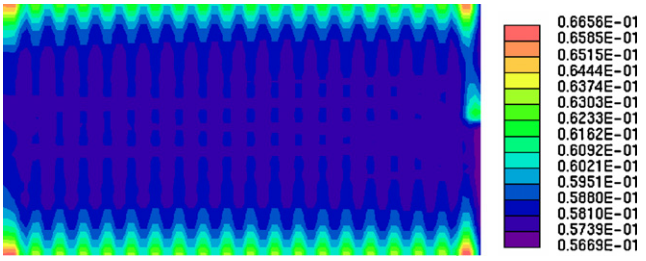

Fig. 13. Distribution of ohmic over-potential.

an air-breathing PEMFC has some particular characteristics in comparison with general PEMFC with external humidification. The anode side is easily dried without humidification, and the sole water source in anode side is water diffusion from cathode side due to water concentration gradient. Fig. 12 is net water molecules per proton flux through the membrane with the defined water transport direction from anode to cathode. Without external humidity, operating in dry anode gas, a certain amount of product water can transports from cathode to anode by back diffusion. While protons migrate from the anode to cathode and carry with them water molecules when current is drawn from the cell. Hence, there is always a little osmotic drag; the amount of water collected at the anode is the balance between the total amount of water back transported and of water transported again to the cathode due to osmotic drag. It is observed that the net water flux is negative because of the presence of back diffusion. And osmotic drag takes place wherever the current density is high because there is more proton transport, and in the other regions, back diffusion takes place. It can be seen the osmotic drag takes place in the region near the channel opening, and the diffusion occurs in the center and anode inlet region. Fig. 13 is voltage losses due to membrane proton transport resistance. The center region is better hydrated due to stronger water back diffusion, and the ohmic losses are consequently low. The regions in the open area of cathode channel have worse water condition due to osmotic drag effect, the region near the anode inlet the ohmic losses are high because pure hydrogen is used as anode reactant.

4. Conclusions

A complex three-dimensional model including detailed heat/mass transfer parameters and phenomena has been developed for an air-breathing PEMFC with real geometry and structure. The model accounts for all major phenomena except phase change. The numerical results for the cell performance are physically consistent and be in good agreement with the experimental data. The effects of the heat and mass transfer under the free convection, and the water transport on the air-breathing PEMFC performance have been investigated through the examinations of distribution of the velocity, temperature, concentration of gas component, dimensionless coefficient for heat and mass transfer analysis, current density and the concentration over-potential. The profound interactions between velocity, temperature, concentration of gas component and current density are clearly shown from the 'calculated results and their analysis'. The capability of the comprehensive model for analyzing and understanding many interacting in an air-breathing PEMFC that cannot be studied experimentally is demonstrated. As the results this model provides more profound insights into the interacting phenomena between heat, mass transfer and electrochemical reactions in the cell. The non-dimensional oxygen transport coefficient (Sh) has been calculated by full N–S function solution. And then a simple equation of Sherwood number has been derived from the sum of the Grashof number and the diffusional Grashof number. This method is very useful to simplify the calculation and to optimize the design of an air-breathing PEMFC. The model provides a computer-aided tool for the design and the optimization of a future air-breathing PEMFC with better performance.

References

[1] C.Y. Chen, P. Yang, J. Power Sources 123 (2003) 37–42.
[2] D. Chu, R.Z. Jiang, J. Power Sources 83 (1999) 128–133.
[3] P.W. Li, T. Zhang, Q.M. Wang, L. Schaefer, M.K. Chyu, J. Power Sources 114 (2003) 63–69.
[4] D.M. Bernadi, M.W. Verbruge, J. Electrochem. Soc. 139 (9) (1992) 2477–2491.
[5] T.V. Nguyen, R.E. White, J. Electrochem. Soc. 140 (8) (1993) 2178–2186.
[6] T.E. Springer, T.A. Zawodzinski, S. Gottesfeld, J. Electrochem. Soc. 138 (August (8)) (1991) 2334–2341.
[7] I.M. Hsing, P. Futerko, Chem. Eng. Sci. 55 (2000) 4209–4218.
[8] S. Dutta, S. Shimpalee, J.W. Van Zee, J. Appl. Electrochem. 30 (2000) 135–146.
[9] S. Dutta, S. Shimpalee, J.W. Van Zee, Int. J. Heat Mass Transfer 44 (2001) 2029–2042.
[10] S.U. Jeong, E.A. Chob, H.-J. Kim, J. Power Sources 159 (2006) 1089–1094.
[11] S.U. Jeong, E.A. Chob, H.-J. Kim, J. Power Sources 158 (2006) 348–353.
[12] J. Ramousse, J. Deseure, O. Lottin, S. Didierjean, D. Maillet, J. Power Sources 145 (2005) 416–427.
[13] E. Arato, P. Costa, J. Power Sources 158 (2006) 200–205.
[14] Y.Y. Shan, S.Y. Choe, J. Power Sources 158 (2006) 274–286.
[15] Y. Wang, J. Ke, W.-Y. Lee, T.-H. Yang, C.-S. Kim, Int. J. Hydrogen Energy 30 (2005) 1351–1361.
[16] Y. Wang, Y.-J. Sohn, W.-Y. Lee, J. Ke, C.-S. Kim, J. Power Sources 145 (2005) 563–571.
[17] Y. Wang, T.H. Yang, W.Y. Lee, J. Ke, C.S. Kim, J. Power Sources 145 (2005) 572–581.
[18] J. Bear, J.M. Buchlin, Modeling and Application of Transport Phenomena in Porous Medium, Kluwer Academic Publishers, Boston, MA, 1991.
[19] S. Um, C.-Y. Wang, K.S. Chen, J. Electrochem. Soc. 147 (12) (2000) 4485–4493.
[20] R.B. Bird, W.E. Stewart, E.N. Lightfoot, Transport Phenomena, second ed., John Wiley & Sons, New York, 2002.
[21] G. Prentice, Electrochemical Engineering Principles, Prentice-Hall Inc., 1991.